CW 100 mA ELECTRON RF GUN FOR NOVOSIBIRSK ERL FEL

V. Volkov#, V. Arbuzov, E. Kenzhebulatov, E. Kolobanov, A. Kondakov, E. Kozyrev, S. Krutikhin, I. Kuptsov, G. Kurkin, S. Motygin, A. Murasev, V. Ovchar, V.M. Petrov, A. Pilan, V. Repkov, M. Scheglov, I. Sedlyarov, S. Serednyakov, O. Shevchenko, S. Tararyshkin, A. Tribendis, N. Vinokurov, BINP SB RAS, Novosibirsk, Russia

Abstract

Continuous wave (CW) 100 mA electron rf gun for injecting the high-quality 300-400 keV electron beam in Novosibirsk Energy Recovery Linac (ERL) and driving Free Electron Laser (FEL) was developed, built, and commissioned at BINP SB RAS. The RF gun consists of normal conducting 90 MHz rf cavity with a gridded thermionic cathode unit. Bench tests of rf gun is confirmed good results in strict accordance with our numerical calculations. The gun was tested up to the design specifications at a test bench that includes a diagnostics beam line. The rf gun stand testing showed reliable work, unpretentious for vacuum conditions and stable in long-term operation. The design features of different components of the rf gun are presented. Preparation and commissioning experience is discussed. The beam test results are summarized.

INTRODUCTION

Recent projects of advanced sources of electromagnetic radiation [1] are based on the new class of electron accelerators where the beam current is not limited by the power of rf system – energy recovery linacs (ERLs). Such accelerators require electron guns operating in continuous wave (cw) mode with high enough average current. The only solution is an rf gun, where the cathode is installed inside the rf cavity. The advantages of the rf guns are higher accelerating field, which is desirable to obtain low beam emittance. It has no problem with degradation of the cathode due to poor vacuum in the gun. The considered rf gun if it be used in the most power Novosibirsk FEL can increase it`s power by one order on magnitude more.

In this paper we describe the beam test results of our low-frequency rf gun (see [2-4]) built as the new electron source for ERL of the Novosibirsk FEL facility (see [5]). Measured rf gun characteristics are in Table 1.

Table 1: Measured rf Gun Characteristics

Name	Value
Average beam current, mA	0.003-100
Bunch energy, keV	100 ÷ 400
Bunch duration (FWHM), ns	0.2 ÷ 2.0
Bunch emittance, mm mrad	10
Bunch charge, nC	0.3 ÷ 3.8
Bunch repetition frequency, MHz	0.01 ÷ 90

#v.n.volkov@inp.nsk.su

RF GUN AND DIAGNOSTIC STAND

Here we shortly describe the rf gun and diagnostic stand presented by sketches of Figs. 1 and 2. Detailed information sees in [2-4]. Perfections of the stand are following: 30 kW water cooled beam dump, 5 cm lead radiation shield, wideband Wall Current Monitor (WCM2), new scheme of cathode-grid modulator with GaN rf transistor, Transition Radiation Sensor, and pair of standard WCM.

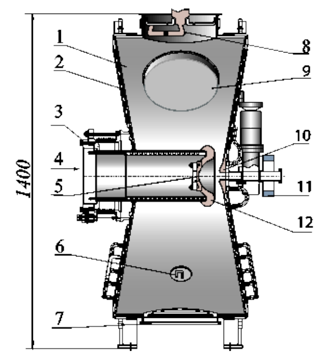

Figure 1: Rf gun sketch.

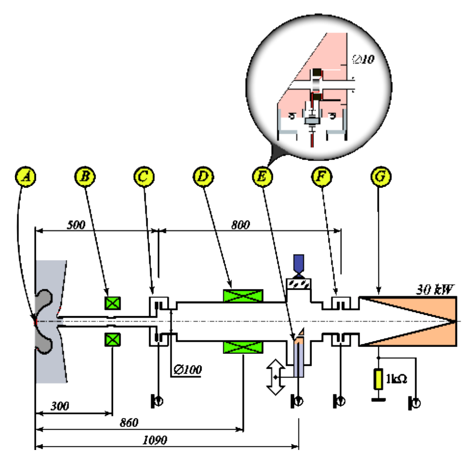

Figure 2: The stand layout.

In figures: 1- Cavity bi-metallic shell; 2-Cavity back wall; 3-Cathode Insert; 4-Cathode injection/extraction channel; 5-Thermionic cathode-grid unit (can be replaced by EIMAC); 6-Loop coupler; 7-Vacuum pumping port; 8-Power input coupler; 9-Sliding tuner; 10-Cone like nose; 11-Peripheral solenoid; 12-Concave focusing electrode.

A-Thermionic cathode-grid unit; B-Emittance compensation solenoid; C-First Wall Current Monitor (WCM1); D-Solenoid ; E-Wideband WCM and transition radiation sensor; F-third WCM; G-Faraday cup and Water-cooled beam dump.

ISBN 978-3-95450-181-6

STAND TESTING RESULTS

Beam Current vs Repetition Frequency

The running for a full beam current is made by repetition frequency rising. There must be changed the bias DC voltage (V_{bias}) on the grid to preserve a bunch charge be constant if it be required. Also bunch charge depends on Modulator pulse voltage (V_{pulse}), the pulse duration (τ_{FWHM}=1÷2 ns), and the heating voltage (V_{heat}, see Fig 3). The last is because the cathode-grid distance is changed inversely of heating power due to the cathode unit thermal elongation. Optimal heating voltage for maximal cathode life time is 14 ÷ 15 V instead of 12.6 V established for rf tubes due to the presence of heat reflected anode surface there.

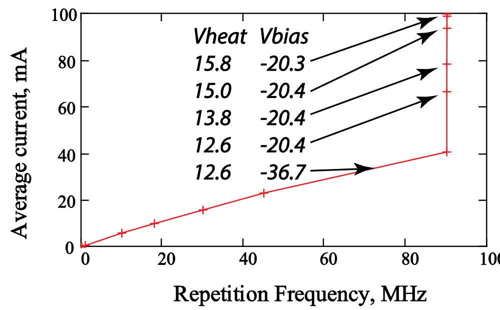

Figure 3: Typical mode of current rising.

Calibration of Cavity Voltage Meter

In order to produce accurate measured data, the calibration of the cavity voltage meter is made with using of two wall current monitors by time delay measuring between them for different cavity voltages. The fitting of measured date by relativistic energy dependency on particle velocity (see Fig.4) gives a perfect accuracy. Numerically calculated beam energy dependency on cavity voltage ($E(keV)=0.9991137 \cdot V(kV)-0.96419$) was used there.

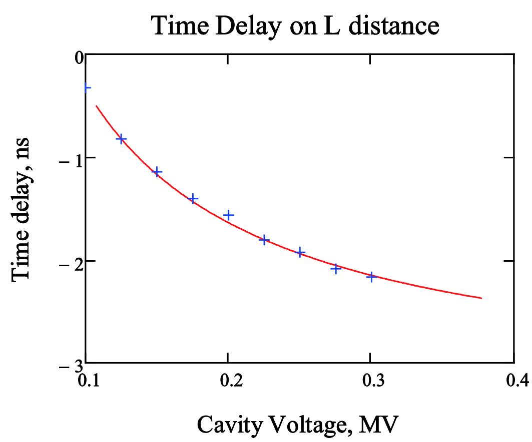

Figure 4: Measured data fitting by theory curve.

Cavity Testing up to 400 kV

The cavity voltage was raised to 400 kV step by step during 5 hours because ½ hour operation time needs to normalize pressure level after the each step (see Fig.5). Then the beam current up to 47 mA limited by maximal beam dump power was getting on in the typical rising mode as shown in Fig. 3.

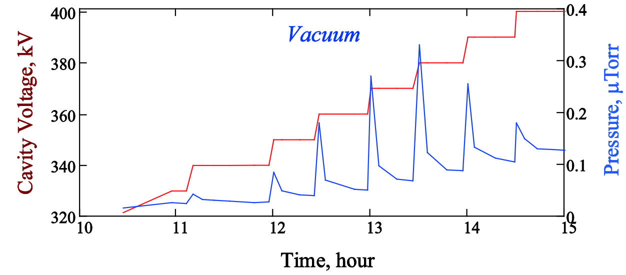

Figure 5: Cavity testing process behavior.

Launch Phase Functions

In order to explain effects of beam bunching, modulator jitter compensation, and other effects in the rf gun, the numerically calculated (by ASTRA cod [6]) launch phase functions are presented. There are launch phase (68°) with maximal bunch energy shown in Fig. 6. At smaller phases, the bunch`s length grow short because its tail having more energy catch up with their head having smaller energy. Also, those bunches launched a little bit earlier/later (jitter) will be late/lead so the jitter will be decreasing.

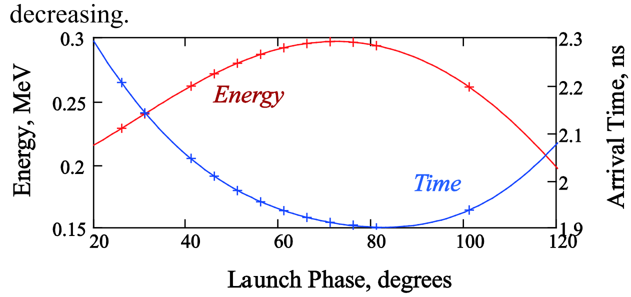

Figure 6: Launch phase functions.

Velocity Modulation Bunching

The numerically calculated r.m.s. bunch duration behaviour on the drift space after the rf gun is presented in Fig.7.

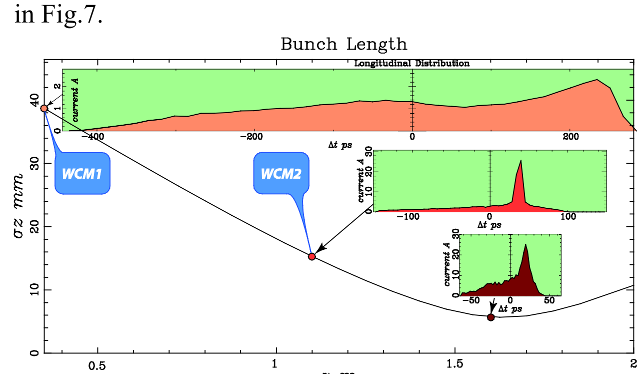

Figure 7: Bunch duration behaviour on the drift space.

Current distributions along bunches are shown by insertions. Frontal spike is formed into cathode-grid gap due to bunching effect there. Then it grows short to be of 20 ps FWHM duration at the distance of 1.1 m where the wide band WCM2 is placed. Unfortunately, our 4 GHz oscilloscope cannot show pulses with τ<200 ps, it all viewed as τ≈200 ps as shown in Fig.8.

ISBN 978-3-95450-181-6

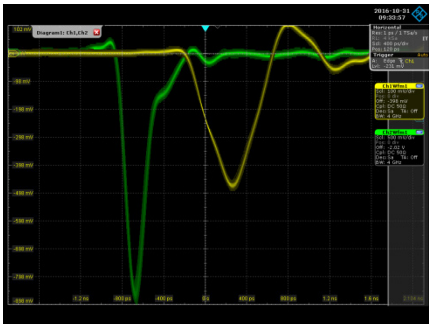

Figure 8: WCM1 (yellow) and WCM2 (green) pulses.

Modulator Jitter Compensation

The jitter compensation effect has confirmed by time delay dependency on launch phase measured between two WCMs with 1.2 m distance (see Fig. 9). Maximal bunch energy is at $\Phi_e=68°$ where it equal to the arrival phase by accurate within some constant. At all other launch phases the arrival phases are behind of it because lower bunch energies (or velocities). Arrival pulse phase becomes independent on Launch phase at $\Phi_j=27°$, i.e. the jitter is compensated there (modulator jitter is ~ $\pm 1\div 2°$).

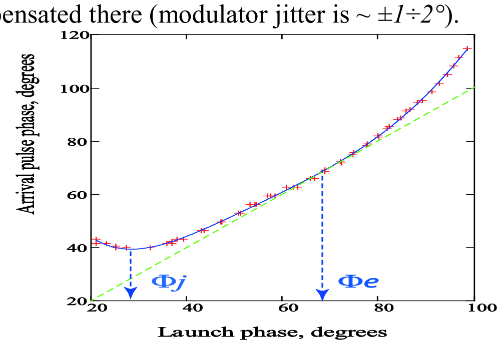

Figure 9: Arrival pulse phase behavior.

Emittance Measurements

Bunch emittance was measured by solenoid focusing method when the spot size of the beam focussed to a target is measured through CCD camera registering the transition radiation. Then the measured data behaviour on the focusing solenoid strength is compared with ASTRA numerically calculated behaviour (see Fig. 10). The deviation is only 9% so we can trust to our calculations.

As the calculation predicts, the measured normalized emittance of ε=15.5 mm mrad can be compensated by a proper solenoid focusing scheme to ε=10 mm mrad.

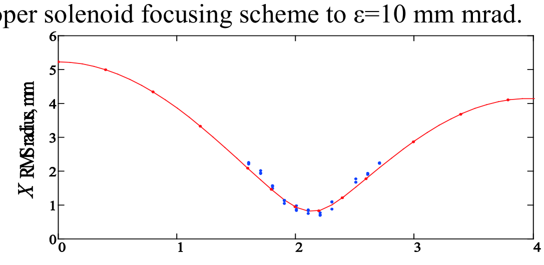

Figure 10: Measured and calculated beam behaviors.

Dark and Leakage Currents

Two places with peak surface field of 10-14 MV/m only can be the sources of field emitted dark currents (see Fig. 11). As we see from Fig. 11, there are no dark currents in the beam absolutely that confirms definitely.

Leakage current source is the cathode oneself at some bias voltages. There is depending on heating voltage because cathode-grid gap depended. To exclude leakage current from the beam we must chose proper bias voltage.

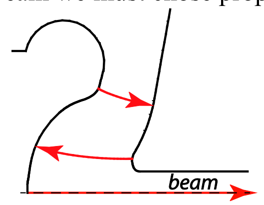

Figure 11: Dark current trajectories in cavity geometry.

Radiation Background

Radiation background was measured during cavity testing from 320 to 400 kV with radiation sensors at 1.5 m. The data exactly coincides with R_{15} is presented in Fig.12 by Fouler-Nordheim (F-N) coordinates in view of straight lines having the enhancement factor of $\beta=628$. The accurate calculations of this field emission process have shown surprisingly things: all calculated values have F-N nature, i.e. have view of straight lines (see Fig. 12) having different β: *I*-dark current, $\beta_I=1250$; P_e-dark current power, $\beta_e=1003$; P_γ-bremsstrahlung power, $\beta_\gamma=865$; R_d-Radiation doze power shielded by Cu with d thickness in mm, $\beta_{3,5,10,15}=721,695,649,628$.

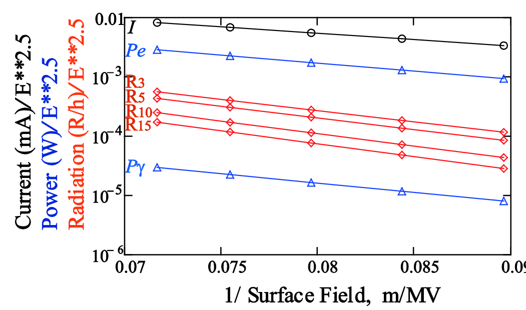

Figure 12: Calculated field emission process.

REFERENCES

[1] Vinokurov, N. A., Levichev, E. B., 2015. Undulators and wigglers for the production of radiation and other applications, Physics-Uspekhi. 58 850–871.

[2] Volkov V.N., et al., First test results of RF gun for the Race-Track Microtron Recuperator of BINP SB RAS. RuPAC2012, 2012, Saint-Petersburg, Russia.

[3] Volkov V., et al., Thermionic cathode-grid assembly simulations for rf guns. PAC2009, 2009, Vancouver, British Columbia, Canada.

[4] V. Volkov, et al., Thermocathode Radio-Frequency Gun for the Budker Institute of Nuclear Physics Free-Electron Laser. ISSN 1547-4771, Physics of Particles and Nuclei Letters, 2016, Vol. 13, No. 7, pp. 827–830.

[5] Kulipanov, et al., Novosibirsk Free Electron Laser—Facility Description and Recent Experiments, IEEE TRANSACTIONS ON TERAHERTZ SCIENCE AND TECHNOLOGY. 5. doi:10.1109/ TTHZ.2015.2453121.

[6] K. Flottmann, ASTRA User`s Manual, http://www.desy.de~mpyflo/Astra_docomentation .

ISBN 978-3-95450-181-6